A&A 466, 697–704 (2007)
DOI: 10.1051/0004-6361:20066549

Astronomy & Astrophysics

Modulation loops, time lag and relationship between cosmic ray intensity and tilt of the heliospheric current sheet

Badruddin[1], M. Singh[2], and Y. P. Singh[1]

[1] Department of Physics, Aligarh Muslim University, Aligarh 202 002, India
e-mail: badr_phys@yahoo.co.in
[2] Department of Physics, Hindustan Institute of Technology, Greater Noida, India
e-mail: ss2008mm@yahoo.co.uk

Received 12 October 2006 / Accepted 26 January 2007

ABSTRACT

Aims. We study certain aspects of the solar modulation of galactic cosmic ray intensity during different solar activity cycles and in different polarity states of the heliosphere.
Methods. We plotted modulation loops between the cosmic ray intensity and the tilt angle of the heliospheric current sheet during three solar activity cycles 21, 22 and 23 and obtained the area of modulation loops. The time lag between the tilt angle and the cosmic ray intensity in odd, even solar activity cycles and during $A > 0$, $A < 0$ polarity states of the heliosphere are determined using correlation analysis. Rate of intensity decrease with tilt angle during different solar and magnetic cycles are estimated from best fit method.
Results. Marked differences during the two odd and the one even solar cycles, as well as during different polarity states of the solar magnetic field ($A > 0$ and $A < 0$) are found. We observe variations in finer features of modulation loops obtained using one, three, six and twelve rotation averaged data. We find that the time lag in even cycle (22) is much different from that in odd cycles (21, 23). Moreover, considerable difference in time lags are also observed during $A > 0$ and $A < 0$ polarity states of the heliosphere. We also find that the cosmic ray intensity decreases at much faster rate (and with better correlation) with increase in tilt angle during $A < 0$ than $A > 0$, indicating stronger response to the tilt angle changes during $A < 0$. These results are discussed in the light of 3D modulation models including the gradient and curvature drifts and the tilt of the heliospheric current sheet.

Key words. cosmic rays – Sun: activity – solar wind – solar-terrestrial relations

1. Introduction

Plots of yearly averaged cosmic ray intensity (CRI) against sunspot number, for a complete solar activity cycle lead to hysteresis or modulation loops. This hysteresis effect in between long-term variation in CRI and solar activity (e.g. sunspots) is known and being studied from quite some time (e.g. Neher & Anderson 1962; Wang 1970). In a study of such modulation loops obtained for different solar cycles, Van Allen (2000) argued that differences in certain features of modulation loops in odd and even cycles give some support to include gradient and curvature drifts in the theories of transport of cosmic rays in the heliosphere. On the basis of his analysis, Van Allen put forward some interpretive remarks. Although he himself suggests that his remarks may not be definitive but expects that his observations will stimulate more detailed consideration of the significance of modulation loops. Some other recent studies about hysteresis effect in long-term cosmic ray modulation include those of Mavromichalaki et al. (1998), Cliver & Ling (2001), Dorman et al. (2001), Usoskin et al. (2001), Ozguc & Atac (2003), Kane (2003), Singh et al. (2005), Sabbah & Rybansky (2006) and Kane (2006a). These studies of modulation loops and time lags use various solar activity indices such as sunspot number (Van Allen 2000), solar flare index (Ozguc & Atac 2003), number of solar flares (Hatton 1980) etc. Although attempts have been made to explain the observed results in terms of the known physical processes, including gradient and curvature drifts, governing the modulation of cosmic ray particles in the three-dimensional heliosphere, there is still a need for understanding and the interpretation of finer details of hysteresis loops during different solar cycles.

To understand how the cosmic rays move in the heliosphere under the influence of gradient and curvature drifts, one needs to recognize the importance of heliospheric current sheet (HCS) that separates the hemispheres of oppositely directed magnetic fields (e.g. see, Kota & Jokipii 1983; Badruddin et al. 1985; Venkatesan & Badruddin 1990; Potgieter et al. 2001; Smith 2001). The angle between the plane of the current sheet and a plane that is an extension of the Sun's equator is referred to as the tilt angle of HCS. As the tilt of the heliospheric current sheet is thought to play central role in drift models of galactic cosmic ray modulation, we attempt to study the time lag, hysteresis effect, area of the hysteresis loop, cosmic ray response to changes in tilt angle during different solar and magnetic conditions, by considering evolution of the heliospheric current sheet during 1976–2006, which includes solar activity cycles 21, 22 and 23.

2. Results

Long-term plots between the cosmic ray intensity and the solar-activity parameters depict a general picture of inverse relationship, and provide a broad qualitative idea about the lead/lag relationship between them. Since the HCS and its evolution in 3D heliosphere is thought to play an important role in cosmic

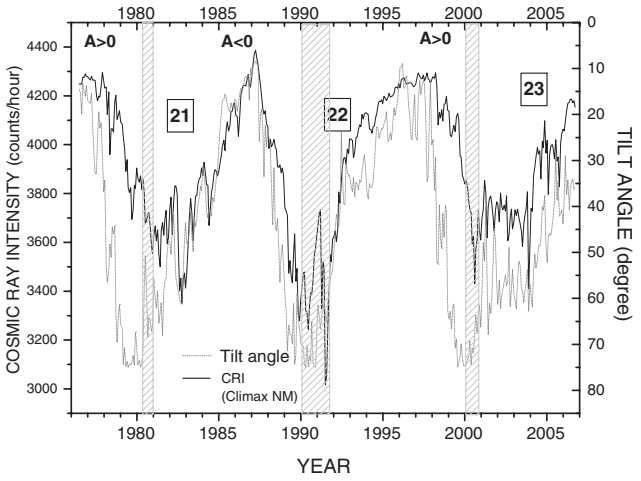

Fig. 1. Changes in cosmic ray intensity, indicated by counting rate (counts/hour with scaling factor 100) of Climax neutron monitor, and tilt angle (in degrees) of the heliospheric current sheet (scale inverted).

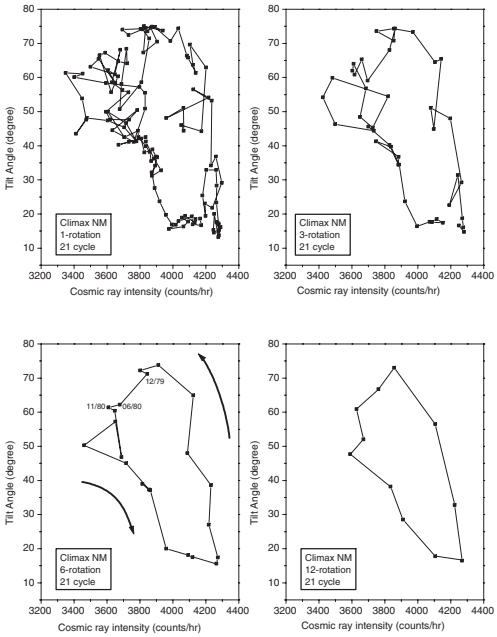

Fig. 2. HCS Tilt angle (in degrees) versus cosmic ray intensity, indicated by counting rate (counts/hour with scaling factor 100) of Oulu neutron monitor, hysteresis plots for solar activity cycle 21; data averaged over 1, 3, 6 and 12 Carrington rotations.

ray modulation, we have plotted in Fig. 1 the time variation of the solar-rotation averaged cosmic ray intensity, measured by Climax neutron monitor (solid line), and tilt angle (dotted line) of the HCS from 1976 to 2006. The periods between two thin vertical lines, shown in the figure around 1980, 1990 and 2000 corresponds to the solar polar magnetic field reversal in solar cycles 21, 22 and 23, respectively. The general (inverse) relationship between the CRI and the tilt angle (TA) of HCS is apparent from this figure. However, the time lag between CRI and TA appears to be different during different solar cycles (odd and even) as well as during different polarity states ($A > 0$ and $A < 0$) of the heliosphere.

Further insight about the relationship between CRI and TA during different phases (increasing, maximum, decreasing, minimum) of a solar activity cycle, and difference in their relationship, if any, during different solar cycles can be obtained by plotting hysteresis diagram (modulation loops) between these parameters in different solar cycles. It is expected that finer details about the modulation may be obtained if one plots these hysteresis diagrams for different time averages (e.g. 1-rotation, 3-rotation, 6-rotation and 12-rotation averages).

Figure 2 shows the cross-plots between cosmic ray intensity recorded at Climax neutron monitor (Rc = 2.97 GV) and tilt angle of the HCS for solar cycle 21. Hourly CRI records of neutron monitor data were averaged over the periods of 1-solar rotation, 3-rotation, 6-rotation and 12-rotation. Corresponding Carrington rotation's tilt angles of the HCS were used to obtain average angles for the tilt for respective periods. Four cross-plots for cycle 21 in Fig. 2 show some interesting features about the time lag between CRI and TA during this solar cycle and, the response of CRI to the TA changes during its different phases.

A general oval shape loop indicates a large time lag between CRI and TA during the solar cycle 21. As regards the effectiveness of HCS tilt in the cosmic-ray modulation, during different phases of the activity cycle, the whole modulation loop (see Fig. 2) can be visualized to indicate (a) slow rate of intensity decrease with increasing TA during increasing phase (weak effect/response); (b) "inverse-modulation" i.e. decrease in CRI with decrease in TA during/around solar maximum and solar polarity reversal (no effect/response); (c) fast rate of intensity decrease with increase in TA during declining phase (strong effect/response); and (d) intensity decreases at a faster rate with TA as solar activity approaches to minimum level (stronger effect/response). Another interesting observation from the cross-plots shown in Fig. 2 is the appearance of "secondary" loops around solar maximum/solar polarity reversal, more clearly seen in 1-rotation and 3-rotation plots, and to some extent in 6-rotation averaged cross-plots.

The HCS divides the heliosphere into two hemispheres of oppositely directed magnetic fields (Smith et al. 1978; Jokipii & Thomas 1981). During the periods when polarity is outward in the northern hemisphere above the HCS and inward in the southern hemisphere below the HCS (referred to as $A > 0$ polarity state of the heliosphere), positively charged particles preferentially enter the heliosphere from the direction of the solar poles. When the polarity is reversed i.e. magnetic field is inward in the northern hemisphere and outward in the southern hemisphere (referred to as $A < 0$ state), positively charged particles approach the sun from along the HCS (e.g. Kota & Jokipii 1983; Venkatesan & Badruddin 1990; Potgieter et al. 2001).

During the increasing phase of solar cycle 21 the heliosphere is in $A > 0$ polarity state and the access route of incoming cosmic rays to the inner heliosphere is through the polar regions. Therefore, these positively charged particles will be less affected by drifts associated with the increase in the tilt angle of the HCS. As a consequence of weak response to changes in tilt angle, intensity decreases at a slow rate with increase in tilt angle. Around solar maximum/polarity reversal, when the tilt of the heliospheric current sheet is $\gtrsim 70°$ (closer to 90°), cosmic ray particles encounter the fields in polar regions of both positive and negative polarities and they drift sometimes inward and sometimes outward (Zhang 2003), resulting in no apparent response to tilt angle changes. However, during/around solar maximum, the heliosphere is filled with Global Merged Interaction Regions (GMIRs) that extend large range of latitude and longitude (Burlaga et al. 1985; McDonald et al. 1993). These GMIRs act as diffusion barriers to the particles and are likely agents responsible for the modulation during solar maximum. Secondary

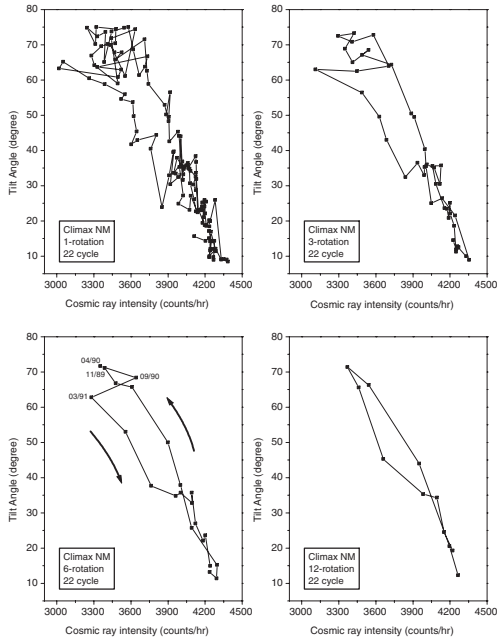

Fig. 3. Same as Fig. 2 for solar cycle 22.

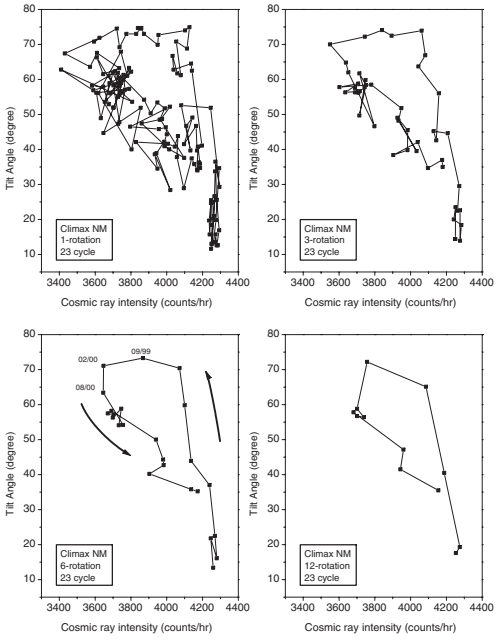

Fig. 4. Same as Fig. 2 for solar cycle 23 (upto September 2006).

loops appearing in the 1 and 3 rotation averaged hysteresis plots in 1978 and 1982, before and after solar maximum, probably correspond to the effects of episodic cosmic ray events observed during these periods. After the polarity reversal around solar maximum, the state of the heliosphere has changed to $A < 0$ when the particle access to the inner heliosphere is via the HCS. In this condition drifting cosmic ray particles will be more readily affected by the changes in the tilt angle resulting in intensity reduction at a fast rate with increase in tilt angle (strong response) during decreasing phase of solar cycle 21. As the solar activity decreases further, and the heliosphere is more conducive for drift effects to be observed, gradient and curvature drifts become more important and the CRI changes at a faster rate with smaller changes in TA (stronger response) even though the intensity is at a lower level.

In Fig. 3 we have shown the cross-plots between the tilt angle and the CRI for the solar cycle 22. These plots correspond to 1, 3, 6 and 12-rotation averaged data. A comparison of cycle 22 modulation loop with that of cycle 21 shows that area of cycle 22 loop is much smaller than that of cycle 21, indicating a smaller time lag between CRI and TA in cycle 22 than 21. Although not as distinct as in cycle 21, some qualitative differences are seen in the response of CRI to the TA changes in cycle 22 also. From the cross-plots shown in Fig. 3 we may infer that during the initial (increasing) phase of solar cycle 22, the response is somewhat stronger than in later (decreasing) phase of solar cycle, more clearly seen in 6-rotation plot in the lower solar activity periods. A short period of "inverse" (or no) relation between CRI and TA around solar maximum/polar field reversal periods in 1990, and a secondary loop around the same period are other features of these plots.

Cross-plots between CRI and TA for cycle 23 (up to 2006) are shown in Fig. 4. A slow rate of decrease in CRI with increase in TA (weak effect/response) during the initial (increasing) phase, a larger intensity decrease without any significant change in TA (almost no relation between CRI and TA) during around solar maximum and polarity reversal, a fast increase in CRI with decrease in TA during decreasing phase of solar cycle 23 is apparent from Fig. 4. These observations, from the cross-plots between CRI and TA for solar cycle 23, are almost similar to those observed in cycle 21 during different phases of the solar cycles; a weak CRI response to TA changes during the increasing phase, almost no-response in and around solar-maximum/polarity-reversal period, and a stronger response during decreasing phase.

To make sure that our observations discussed above, are neither incidental nor observable at any particular neutron monitor/location only, we have used CRI data of one more neutron monitor, located at Oulu, whose cutoff rigidity is 0.77 GV. Adopting similar procedure and criteria as discussed above, we have obtained cross-plots between Oulu NM intensity and tilt angle of the HCS. These plots for solar cycles 21, 22 and 23 are shown in Figs. 5–7, respectively. It is clearly seen that these plots with Oulu NM data are similar to those obtained with Climax NM data in respective solar cycles.

Although long-term (e.g. Fig. 1) and hysteresis plots (e.g. Figs. 2–4 and 5–7) provide qualitative informations about the time lag between CRI and TA, response of CRI variations to TA changes and the area of modulation loops during different solar-activity and solar magnetic conditions, their quantitative estimate will provide further insight about the modulation process.

To determine the time lag between CRI and TA in solar cycles 21, 22 and 23, we have calculated the correlation coefficients between the TA of HCS and Carrington rotation averages of CRI, by introducing successively time lags of 0 to 29 Carrington rotations. The time lag (in Carrington rotation) versus the correlation coefficient graphs for the three solar cycles are plotted in Fig. 8. From the optimum value of the correlation coefficient, it is inferred that the time lag is 24 Carrington rotations during the odd solar cycle 21 (see also Table 1). On the other hand, the time lag during even cycle 22 is much smaller (1–2 Carrington rotations). The time lag between TA and CRI during other odd cycle 23 is again found to be large (12–14 Carrington rotations).

It may be worth mentioning that the time lag is larger, in odd cycles 21 and 23, when the recovery phase of the ~11 year modulation cycle lies in $A < 0$ epochs; in this polarity state, positively charged particles enter the heliosphere via the HCS. The time lag is much smaller in even solar cycle cycle 22, when

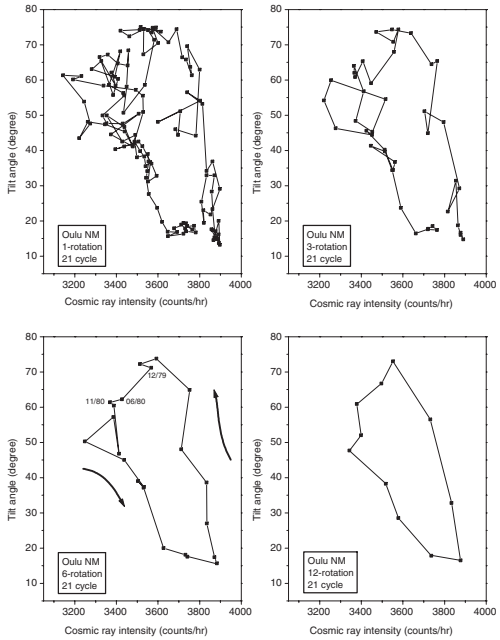

Fig. 5. HCS Tilt angle (in degrees) versus cosmic ray intensity, indicated by counting rate (counts/hour with scaling factor 100) of Oulu neutron monitor, for cycle 21; data averaged over 1, 3, 6 and 12 Carrington rotations.

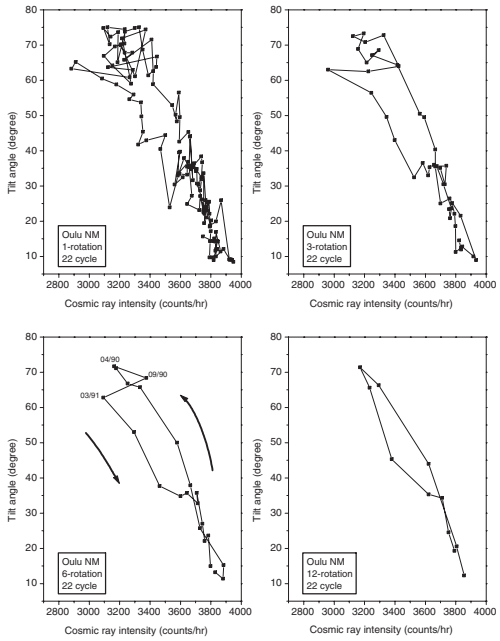

Fig. 6. Same as Fig. 5 for solar cycle 22.

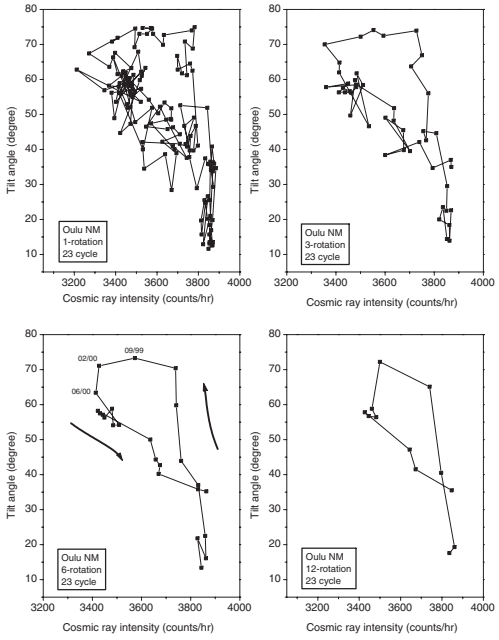

Fig. 7. Same as Fig. 5 for solar cycle 23.

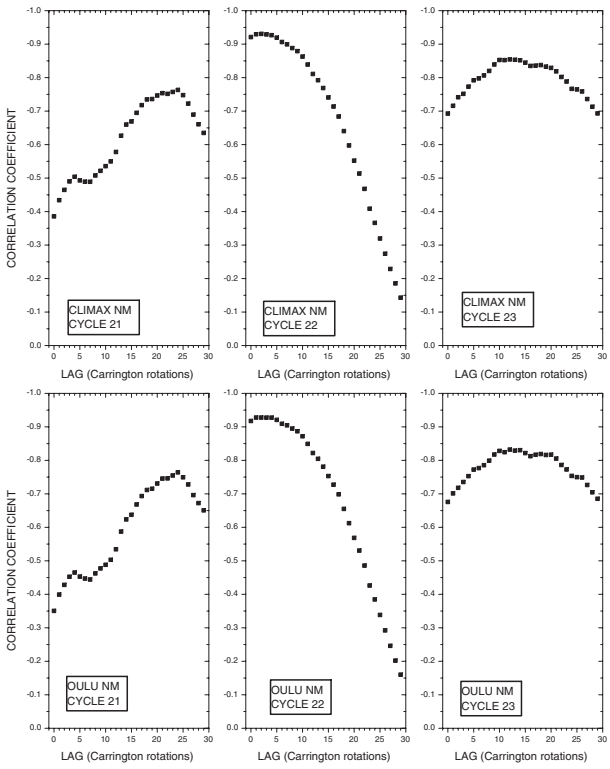

Fig. 8. Lag correlation coefficients between tilt angle and GCR intensity (Climax and Oulu NM) for cycle 21, 22 and 23.

the recovery phase of the ∼11 year modulation cycle lies in $A > 0$ polarity state and the access of cosmic ray particles to the inner heliosphere is through solar polar regions. This observation motivated us to calculate the time lag between CRI and TA during two polarity epochs $A < 0$ (1982–89) and $A > 0$ (1991–99), by adopting the same procedure as that used for obtaining the time lags during the solar cycles 21, 22 and 23. These results are plotted in Fig. 9. It is seen from this figure that the time lag is ∼10–11 Carrington rotations during $A > 0$ and it is only 3 rotation periods in $A < 0$ (see also Table 2). To make sure that these results were not obtained by any chance, we have calculated time lags using data of two neutron monitors at Climax and Oulu having different cut off rigidities.

From Figs. 2, 3 and 5, 6, we have observed that the area of odd-cycle modulation loop (21) is much larger than that of the even-cycle loop (22). To quantify this difference, we have estimated the loop area of individual solar cycles from six-rotation averaged plot of TA versus CRI, both for Climax and Oulu neutron monitor count rates. These estimates are given in Table 3. It is found that the area of the modulation loops of both the odd

Table 1. Time lag between TA and CRI in different solar cycles and correlation coefficient *r*.

Solar cycle	NM station	Time lag (Carrington rotations)	Maximum value of "*r*"
21	Climax	24	–0.76
	Oulu	24	–0.76
22	Climax	02	–0.93
	Oulu	01	–0.93
23	Climax	12	–0.85
	Oulu	14	–0.83

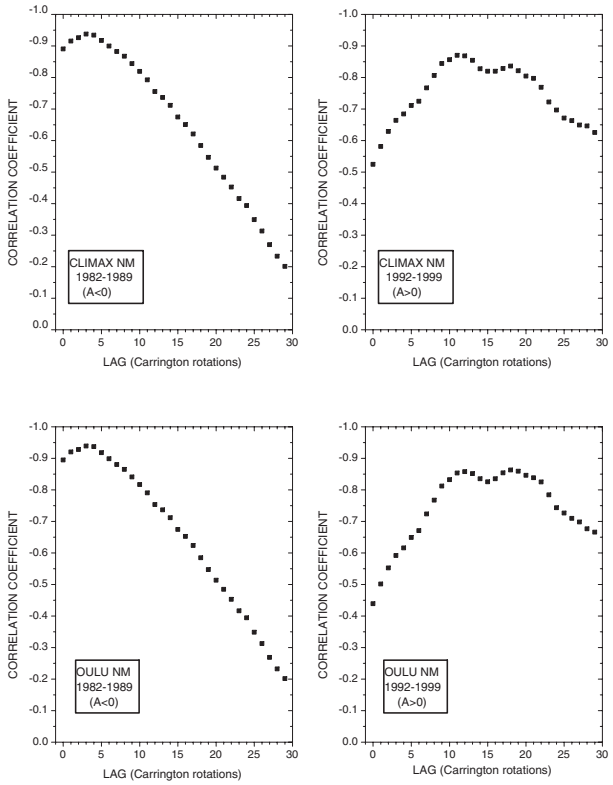

Fig. 9. Lag correlation coefficients between TA and GCR intensity (Climax and Oulu NM) during $A < 0$ and A> 0 polarity epochs.

cycle 21 is about three times larger than the area of the loop for even cycle 22. However, cycle 23 area is not as larger as 21; an indication from the data upto 2006.

We presented earlier, in this paper, a qualitative discussion about the cosmic-ray response/effectiveness to TA changes during different phases of solar activity cycle (minimum, increasing maximum and decreasing phases), and during different polarity states of the heliospheric magnetic field ($A < 0$ and $A > 0$). To elaborate it further, we did correlation analysis between 6-rotation averaged data of CRI and TA and estimated, from the linear fit to the data, the rate of intensity change with the change in tilt angle ($\Delta I/\Delta\Lambda$) of the HCS.

To estimate $\Delta I/\Delta\Lambda$, during different solar cycles and polarity states and, at the same time, ensuring that the solar activity conditions are not much different in periods considered during different solar cycles, we did correlation analysis during initial (increasing) phase of solar cycles 21, 22 and 23. The results of the analysis are given in Table 4. It is evident from tabulated values that the intensity decreases at much faster rate (2 to 3 times) with tilt angle change during even cycle (22) than the odd cycles (21, 23). It is to be mentioned here that increasing phase

Table 2. Time lag between TA and CRI in different polarity states ($A < 0$, $A > 0$).

Solar cycle	NM station	Time lag (Carrington rotations)	Maximum value of "*r*"
21	Climax	24	–0.76
	Oulu	24	–0.76
22	Climax	02	–0.93
	Oulu	01	–0.93
23	Climax	12	–0.85
	Oulu	14	–0.83

Table 3. Area of TA versus CRI modulation loops; cycle 23 value is approximate.

Cycle	Area$\times 10^5$	
	Climax NM	Oulu NM
21	23.559	18.493
22	7.778	7.326
23	11.016	7.420

Table 4. Rate of intensity decrease with tilt angle ($-\Delta I/\Delta\Lambda$) during initial (increasing) phase of solar cycles (6-rotation averaged data).

Solar cycle and phase	Period	Solar polarity (A)	$-\Delta I/\Delta\Lambda$ Climax NM	Oulu NM
21 ↑	1976–79	>0	669.2	380.5
22 ↑	1987–89	<0	1447.8	1864.8
23 ↑	1997–99	>0	527.9	667.1

of even cycle 22 lies in $A < 0$ epoch and those of odd cycles 21 and 23 in $A > 0$ epoch; the access route of cosmic ray particles is different in two polarity epochs (via equatorial/polar regions).

To understand whether the particle access route to the inner heliosphere is the main cause that makes this difference in responsiveness of the tilt of the HCS, we did regression analysis by separating the data periods into two groups namely $A > 0$ and $A < 0$ polarity epochs, irrespective of the solar cycles and their epochs (of course, periods of polarity reversal and very high solar activity periods are excluded). Figures 10–11 and 12–13 show the results of these analyses. The slopes of these curves giving the rate of intensity decrease with change in tilt angle, along with the correlation coefficients are given in Table 5.

We find that the response of CRI to the changes in the tilt of HCS is about twice as large during $A < 0$ than $A > 0$. Further, correlation between the CRI and TA is better during $A < 0$ than $A > 0$. Correlation analysis during the initial phases of solar activity cycle 21 ($A > 0$), 22 ($A < 0$) and 23 ($A > 0$) discussed earlier (see Table 4) show essentially these differences in the response to tilt angle change during $A > 0$ and $A < 0$ epochs.

The development and evolution of present odd cycle 23 bears resemblance to odd cycles (e.g. 19, 21) in some respect and to even cycles (20, 22) in some other respect. For example, Ozguc & Atac (2003) found that current solar cycle 23 develops in a way which is generally similar to even numbered cycle 20. It has also been reported in the recent past (Dmitriev et al. 2002) that heliospheric quantities during rising phase of current cycle 23, in general, follow the averages and deviations of cycle 20. On the other hand, Van Allen (2000) and Cliver & Ling (2001) reached at the conclusion that early phase of cycle 23 bears more resemblance to those of earlier odd cycles 19 and 21 (see also Kane 2006b; Singh et al. 2006).

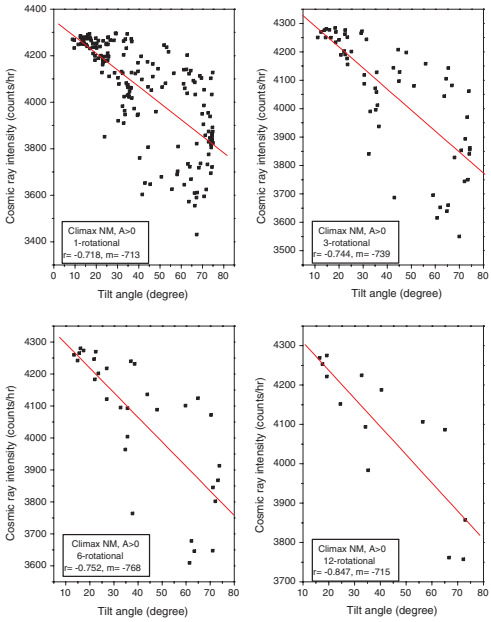

Fig. 10. Scatter plots and best fit curves between TA and GCR intensity (Climax NM) for 1, 3, 6 and 12 rotation averaged data during $A > 0$ epoch, correlation coefficients (r) and slopes (m) for each fitted curve are also given.

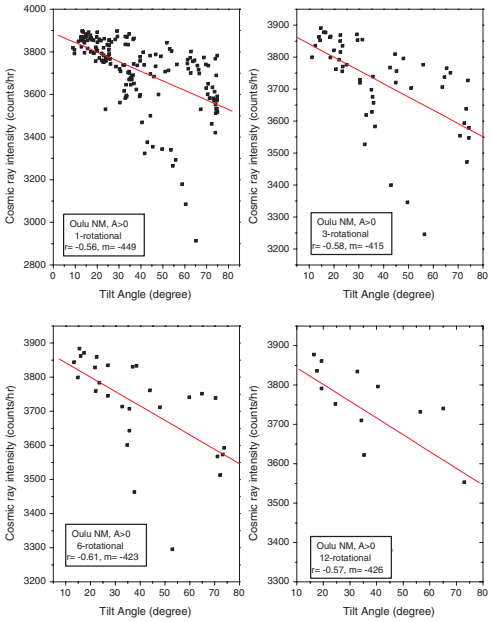

Fig. 12. Scatter plots and best fit curves between TA and GCR intensity (Oulu NM) for 1, 3, 6 and 12 rotation averaged data during $A > 0$ epoch, correlation coefficients (r) and slopes (m) for each fitted curve are also given.

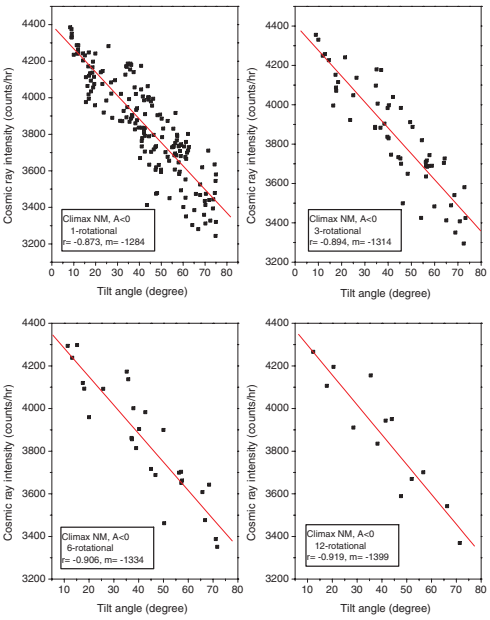

Fig. 11. Same as Fig. 10 during $A < 0$ polarity epoch.

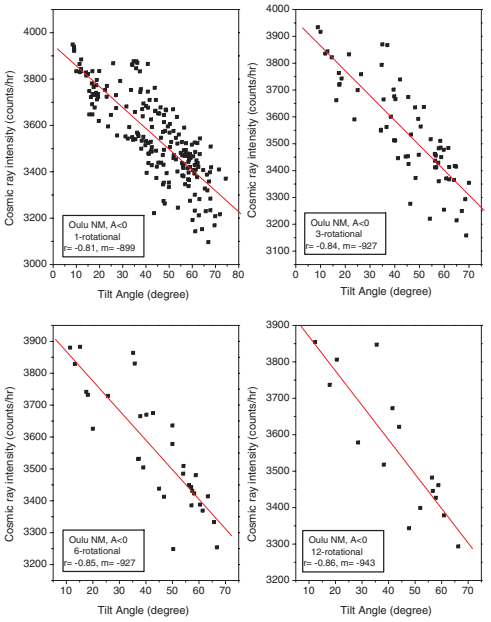

Fig. 13. Same as Fig. 12 during $A < 0$ epoch.

We have looked at the similarity/dissimilarity between (a) the odd cycles 23 and even cycle 22 (b) odd cycles 23 and 21, from CRI-modulation point of view. For this purpose we have compared the CRI versus TA modulation loops of (a) cycle 23 with that of 22 (Figs. 14, 16) and (b) cycle 23 with that of cycle 21 (Figs. 15, 17) using data of Climax & Oulu neutron monitors. We observe that the two odd cycle (21 and 23) loops resemble not only during early phase but during the maxima of the two cycles also. On the other hand, the evolution of cycle 22 and 23 loops appears quite different during early and maximum phase of these two cycles. It is to be mentioned here that the tilt angle in September 2006 was around 35°. However, it will be interesting to see the final shape and loop area of cycle 23 if and when tilt angle decreases further and reaches ∼10° or so.

3. Discussion and conclusions

An essential component of the heliosphere is its current sheet. It separates the heliosphere into two magnetic regions of opposite polarity. When the polarity of the solar magnetic field is outward in the northern hemisphere (above the HCS) and inward in the southern hemisphere (below the HCS), we refer it as $A > 0$ epoch. The heliosphere was in such a polarity state, for example, during seventies (∼1971–1979) and nineties (∼1991–1999). As the solar polarity reverses at/around every solar maximum of

Table 5. Rate of cosmic ray intensity decrease with tilt angle ($-\Delta I/\Delta\Lambda$) during $A > 0$ and $A < 0$, obtained with data averaged over 1, 3, 6 and 12 rotations.

Averaged rotations	Polarity state	Climax NM $-\Delta I/\Delta\Lambda$	Climax NM r	Oulu NM $-\Delta I/\Delta\Lambda$	Oulu NM r
1	$A > 0$	713	–0.72	449	–0.56
	$A < 0$	1284	–0.87	899	–0.81
3	$A > 0$	739	–0.74	415	–0.58
	$A < 0$	1314	–0.89	927	–0.84
6	$A > 0$	768	–0.75	423	–0.61
	$A < 0$	1334	–0.91	927	–0.85
12	$A > 0$	715	–0.85	426	–0.57
	$A < 0$	1399	–0.92	943	–0.86

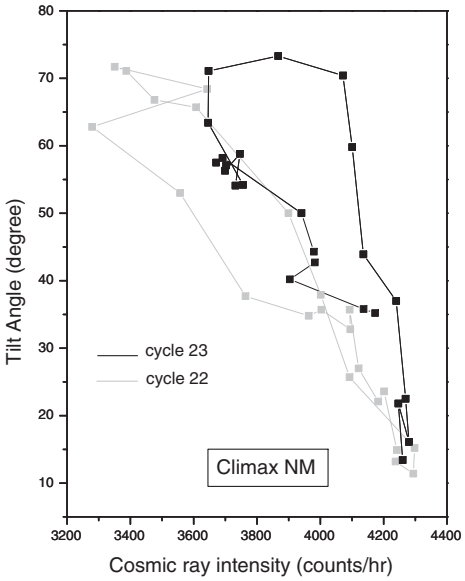

Fig. 14. Comparison of TA vs. GCR intensity (Climax NM) hysteresis curves for solar cycle 22 and 23 (upto September 2006); data averaged over 6-Carrington rotations.

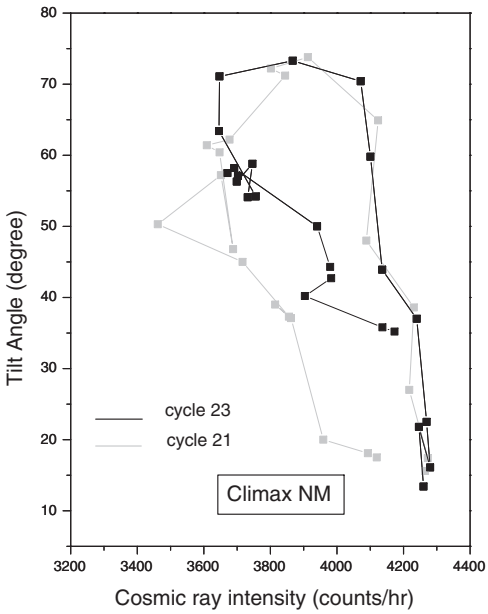

Fig. 15. Comparison of TA vs. GCR intensity (Climax NM) hysteresis curves for solar cycle 21 and 23 (upto September 2006).

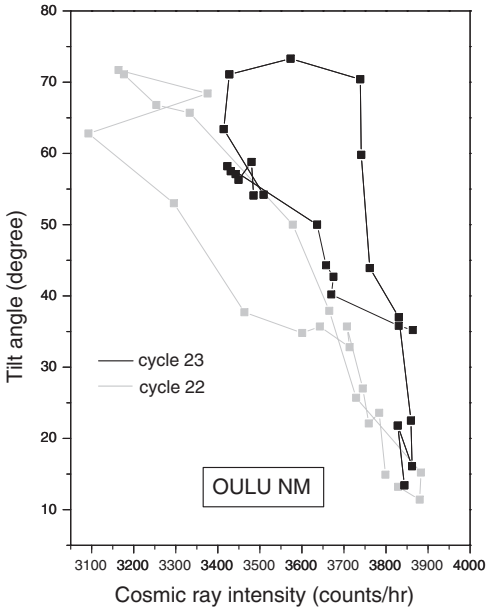

Fig. 16. Comparison of TA vs. GCR intensity (Oulu NM) hysteresis curves for solar cycle 22 and 23 (upto September 2006).

the solar activity cycle, the polarity state of the heliosphere also changes; its magnetic field became inward above the HCS and outward below the HCS. This state of the heliosphere, referred to as $A < 0$ epoch existed during eighties (∼1981–1989) and again the heliosphere is, at present (2006), in negative state.

An essential prediction of the drift theory of cosmic ray modulation is that the cosmic rays (positively charged particles) preferentially enter the heliosphere from the direction of solar poles during $A > 0$ periods and approach the sun from along the HCS during $A < 0$ periods. Cosmic ray particle reach earth more easily when they enter the heliosphere by polar regions (as in $A > 0$ epoch) than when their access route to the inner heliosphere is along the wavy HCS (as in $A < 0$ epoch). In $A < 0$ state, the route of access becomes longer due to waviness of the HCS, the time lag is expectedly longer.

During odd cycles, increasing phase of solar activity cycle lies in $A > 0$ state when particle access to the inner heliosphere is via polar regions. As the odd-numbered cycle progresses, intensity decreases at a slow rate during $A > 0$; in this epoch the current sheet is less effective as positively charged particles enter the heliosphere through polar regions. When the solar activity becomes substantially high, the heliosphere is likely to be filled up with interaction regions extending to large extent in latitude and longitude. These GMIRs will act as barriers to the particles and thus efficiently reducing the cosmic ray intensity when the solar activity is high. Around solar maximum time when the tilt of the HCS is close to 90°, the charged particles will come across the fields of both positive and negative polarities in polar regions and they drift sometimes inward and sometimes outward (Zhang 2003). In such condition, tilt angle of the HCS is unlikely to play an effective role in modulation. After the polarity reversal around solar maximum, the state of the heliosphere changes to $A < 0$ when particle access is along the current sheet. Although presence of interaction regions around the solar maximum may not be conducive for drifts, their limited presence, and drifts along the current sheet, probably accelerates the rate of decrease in intensity. Further as the solar activity decreases toward minimum, the tilt of the HCS decreases and the intensity recovers.

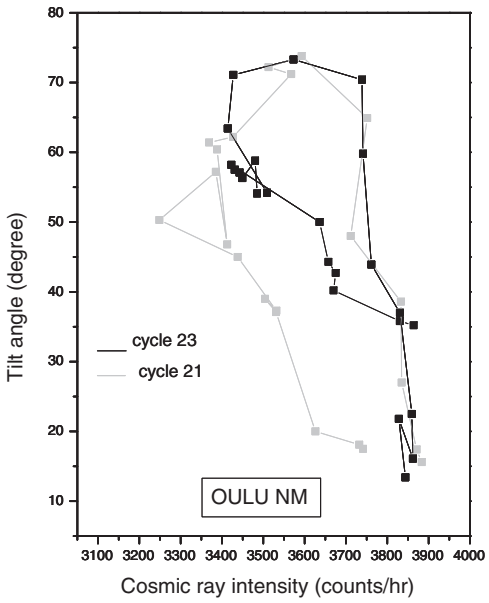

Fig. 17. Comparison of TA vs. GCR intensity (Oulu NM) hysteresis curves for solar cycle 21 and 23 (upto September 2006).

In the even-numbered cycles, the early phase of intensity decrease lies during $A < 0$ polarity state. As the cycle progresses, tilt angle gradually increases and the HCS being more effective due to particle access along the current sheet, intensity decreases at a faster rate. Around solar maximum additional effect of diffusive barriers further reduce the intensity. At solar maximum when the current sheet tilt is close to 90° drift is sometimes inwards and sometimes outwards and diffusive barriers of interaction regions appears to be the main agents responsible for cosmic ray modulation. After polarity reversal around solar maximum, the heliosphere comes to $A > 0$ state when the particle access is via polar regions. Particle access via solar poles, together with diffusive barriers being less effective in this situation, contribute to quick intensity increase (recovery) after solar maximum without much time lag.

Faster rate of CRI decrease with tilt angle change during $A < 0$ than $A > 0$ can also be explained by considering drifts to be dominant process in solar modulation. During $A < 0$ particle access is via current sheet while their access is via poles during $A > 0$. Consequently, drift effects are enhanced and are much effective during $A < 0$ than $A > 0$. If the rate of diffusion does not depend on the polarity of the solar magnetic field, drifts provide a natural explanation for these observations.

Finally, so far as the response of TA change to CRI variation is concerned i.e. from modulation point of view, current solar activity cycle (23) is similar to earlier odd cycle 21, but evolutions of cycle 23 and 22 appear quite different from each other.

Acknowledgements. We thank Cliff Lopate for Climax NM, Ilya Usoskin for Oulu NM, and Todd Hoeksema for HCS data. We thank the referee for constructive comments.

References

Badruddin, Yadav, R. S., & Yadav, N. R. 1985, Planet. Space Sci., 33, 191
Burlaga, L. F., McDonald, F. B., Goldstein, M. L., & Lazarus, A. J. 1985, J. Geophys. Res., 90, 12027
Cliver, E. W., & Ling, A. G. 2001, ApJ, 551, L189
Dmitriev, A. V., Suvorova, A. V., & Veselovsky, I. S. 2002, Adv. Space Res., 29, 475
Dorman, L. I., Dorman, I. V., Iucci, N., et al. 2001, Adv. Space Res., 27, 589
Hatton, C. J. 1980, Sol. Phys., 66, 159
Jokipii, J. R., & Thomas, B. T. 1981, ApJ, 243, 1115
Kane, R. P. 2003, J. Geophys. Res., 108, 1379
Kane, R. P. 2006a, Sol. Phys., 236, 207
Kane, R. P. 2006b, J. Atmos. Solar-Terr. Phys., 68, 1291
Kota, J., & Jokipii, J. R. 1983, ApJ, 265, 573
Mavromichalaki, H., Belehaki, A., & Rafios, X. 1998, A&A, 330, 764
McDonald, F. B., Nand Lal, & McGuire, R. E. 1993, J. Geophys. Res., 98, 1243
Neher, H. V., & Anderson, H. R. 1962, J. Geophys. Res., 67, 1309
Ozguc, A., & Atac, T. 2003, New Astron., 8, 745
Potgieter, M. S., Burger, R. A., & Ferreira, S. E. S. 2001, Space Sci. Rev., 97, 295
Sabbah, I., & Rybansky, M. 2006, J. Geophys. Res., 111, No. A1, A01105
Singh, M., Badruddin, & Ananth, A. G. 2005, Proc. Int. Conf. Cosmic Rays 29th, 2, 139
Singh, M., Singh, Y. P., & Badruddin 2006, J. Geophys. Res., submitted
Smith, E. J., Tsurutani, B. T., & Rosenberg, R. L. 1978, J. Geophys. Res., 83, 717
Smith, E. J. 2001, J. Geophys. Res., 106, 15819
Usoskin, I. G., Marsula, K., Kananan, H., & Kovatsov, G. A. 2001, Adv. Space Res., 27, 571
Van Allen, J. A. 2000, Geophys. Res. Lett., 27, 2453
Venkatesan, D., & Badruddin 1990, Space Sci. Rev., 52, 121
Wang, J. R. 1970, ApJ, 160, 261
Zhang, M. 2003, Adv. Space. Res., 32, 603